

Capacitance and charging of metallic objects

Titus Sandu

*National Institute for Research and Development in Microtechnologies-IMT, 126A, Erou
Iancu Nicolae Street, 077190, Bucharest, ROMANIA*

George Boldeiu

*National Institute for Research and Development in Microtechnologies-IMT, 126A, Erou
Iancu Nicolae Street, 077190, Bucharest, ROMANIA*

Victor Moagar-Poladian

*National Institute for Research and Development in Microtechnologies-IMT, 126A, Erou
Iancu Nicolae Street, 077190, Bucharest, ROMANIA*

Abstract

The capacitance of arbitrarily shaped objects is reformulated in terms of the Neumann-Poincaré operator. Capacitance is simply the dielectric permittivity of the surrounding medium multiplied by the area of the object and divided by the squared norm of the Neumann-Poincaré eigenfunction that corresponds to its largest eigenvalue. The norm of this eigenfunction varies slowly with shape changes and allows perturbative calculations. This result is also extended to capacitors. For axisymmetric geometries a numerical method provides excellent results against finite element method results. Two scale-invariant shape factors and the capacitance of nanowires and of membrane in biological cells are discussed.

Keywords: Capacitance, Laplace equation, Neumann-Poincaré operator, Boundary intergral equation, Localized surface plasmon resonances, Dielectric spectra of live cells

PACS: 41.20.Cv, 82.47.Uv, 87.19.rf, 87.50.C-

Email addresses: titus.sandu@imt.ro (Titus Sandu),
tel:+40-21-269.07.70/ext.30 (Titus Sandu), fax:+40-21-269.07.72 (Titus Sandu)

1. Introduction

Since the 19th century potential theory has been growing continuously as gravitational and electromagnetic interactions and forces were derived from potentials satisfying Laplace, Poisson and Helmholtz equations. Some boundary value problems such as the Dirichlet problem and the Neumann problem, the electrostatic distribution of charges on conductors or the Robin problem can all be defined in terms of potential theory. For domains with sufficiently smooth boundaries the above problems use specific types of potentials like the volume potential, the single- and the double-layer potentials, the logarithmic potential for two-dimensional domains, etc. [1, 2].

The Dirichlet and Neumann problems defined on domains with sufficiently smooth boundaries (i.e., a regular piecewise Lyapunov surface [3]) can be recast in integral equations which lead to compact operators on domain boundary: the Neumann-Poincaré operator and its adjoint [1, 2]. These methods are successfully applied in some practical and physical problems regarding dielectric heterogeneous systems [4] like radio-frequency and microwave dielectric spectra of living cells [5] and plasmonic properties of metallic nanoparticles [6, 7, 8].

Another problem which stems from potential theory is the equilibrium charge distribution on a conductor (the Robin problem) [9] and the implicit capacitance with applications in computational biophysics [10], in scanning probe microscopy [11, 12], or in electrical charge storage in supercapacitors [13]. The capacitance of an arbitrarily shaped body is directly related to hydrodynamic friction and to diffusion-controlled reaction rate [14]. Thus a method of calculating the capacitance is based on “mimicking” the diffusion-controlled reaction rate on an object of arbitrary shape as random walks [15]. Another random walk method is defined just on the boundary and is given by the ergodic generation of the equilibrium charge distribution [16].

A standard procedure for solving the Laplace equation is the Finite Element Method (FEM) [17] and the Boundary Integral Equation (BIE) method which leads to a finite element formulation as the Boundary Element Method (BEM) [18]. In the FEM the entire domain is discretized by using elements and the associated basis functions, while in the BEM only the surfaces of the inclusions within the domain are used for discretization. The bounded and the unbounded domains are on equal footing in the BEM. On the other hand, the FEM solves the static and quasi-static electromagnetic field problems in unbounded domains by using one of the additional ingredients: infinite ele-

ments [19], coordinate transformations [20], or hybrid FEM/BEM methods [21]. Infinite domains can be elegantly and efficiently treated with the hybrid Trefftz method, where, beside the usual elements, an additional set of functions is employed to treat singularities and infinities [22].

In this paper, by a BIE method [23, 24, 25], we will define the capacitance and the equilibrium charge of an arbitrarily shaped object in terms of the eigenvectors of the Neumann-Poincaré operator and of its adjoint [1, 2]. Compared to other methods the operator based BIE method provides directly the geometric dependence of capacitance that is incorporated in an eigenvector norm of the Neumann-Poincaré operator. This eigenvector corresponds to the largest eigenvalue. Accordingly, capacitance is obtained concurrently with other physical properties like localized plasmon resonances of metallic nanoparticles that have the same shape [6, 7, 8]. Furthermore, operator perturbations on eigenvalues and on eigenvectors permit the perturbative estimation of capacitance and other physical properties. The reformulation of capacitance allows defining several scale-invariant shape factors that can also be readily used in the estimation of capacitance for arbitrary shapes. Applications regarding the capacitance of a general capacitor, the membrane capacitance of living cells, charge storage in supercapacitors, and the electric capacitance of molecular nanowires are discussed.

The paper is organized as follows. The method is described in the second section. Then, the connection with a general capacitor is made in the following section. Section 4 describes the numerical method, its accuracy and some applications. The conclusions are summarized in the last section.

2. The operator approach in potential theory. Capacitance of a metallic object

We assume an arbitrarily shaped domain Ω of volume V and bounded by the surface Σ . We denote the complementary set of Ω by $\Omega^c = \mathfrak{R}^3 \setminus \bar{\Omega}$, where $\bar{\Omega}$ is the closure of Ω and \mathfrak{R}^3 is the Euclidian 3-dimensional space. The following operators can be defined on Σ :

$$\hat{M}[u] = \frac{1}{4\pi} \int_{\mathbf{x}, \mathbf{y} \in \Sigma} \frac{u(\mathbf{y}) \mathbf{n}(\mathbf{x}) \cdot (\mathbf{x} - \mathbf{y})}{|\mathbf{x} - \mathbf{y}|^3} d\Sigma(\mathbf{y}), \quad (1)$$

its adjoint,

$$\hat{M}^\dagger [v] = \frac{1}{4\pi} \int_{\mathbf{x}, \mathbf{y} \in \Sigma} \frac{v(\mathbf{y}) \mathbf{n}(\mathbf{y}) \cdot (\mathbf{x} - \mathbf{y})}{|\mathbf{x} - \mathbf{y}|^3} d\Sigma(\mathbf{y}), \quad (2)$$

which is the Neumann-Poincaré operator [2], and the symmetric and non-negative Coulomb operator

$$\hat{S}[u] = \frac{1}{4\pi} \int_{\mathbf{x}, \mathbf{y} \in \Sigma} \frac{u(\mathbf{y})}{|\mathbf{x} - \mathbf{y}|} d\Sigma(\mathbf{y}). \quad (3)$$

In Eqs. (1)-(2) \mathbf{n} is the normal vector to Σ . The operator \hat{M} can be made symmetric via the Plemelj's symmetrization principle $\hat{M}^\dagger \hat{S} = \hat{S} \hat{M}$ [2]. Thus, the operator \hat{M} is symmetric with respect to the inner product defined by the symmetric and non-negative operator \hat{S}

$$\langle v | u \rangle_S = \langle v | \hat{S}[u] \rangle, \quad (4)$$

where $\langle | \rangle$ defines the standard inner product on $L^2(\Sigma)$ and $\langle | \rangle_S$ is the inner product determined by \hat{S} . The Hilbert space $L^2(\Sigma)$ is the vector space of all square-integrable functions defined on Σ . The standard inner product on $L^2(\Sigma)$ of two functions $u_1(\mathbf{x})$ and $u_2(\mathbf{x})$ is defined as

$$\langle u_1 | u_2 \rangle = \int_{\mathbf{x} \in \Sigma} u_1^*(\mathbf{x}) u_2(\mathbf{x}) d\Sigma(\mathbf{x}), \quad (5)$$

where the star sign * signifies the complex conjugate of a complex number. The operators \hat{M} and \hat{M}^\dagger have the same spectrum bounded by the interval $[-1/2, 1/2]$ and the eigenfunctions u_i of \hat{M} are related to the eigenfunctions v_i of \hat{M}^\dagger by $v_i = \hat{S}[u_i]$, which makes them bi-orthogonal, i.e. if $\hat{M}[u_i] = \chi_i u_i$ and $\hat{M}^\dagger[v_j] = \chi_j v_j$, then $\langle v_j | u_i \rangle = \delta_{ij}$ [6, 2, 23]. In physical terms $\hat{M}[u]$ is related to the normal component of the electric field that is generated by surface charge density u . On the other hand, v_i is the electric potential generated on surface Σ by the charge distribution u_i . The largest eigenvalue of \hat{M} and \hat{M}^\dagger is $1/2$ irrespective of the domain shape and its corresponding eigenfunction v_1 of \hat{M}^\dagger is a constant function, i. e., $v_1 = \text{constant}$ on Σ , which comes from the following relation [2]

$$\hat{M}^\dagger [v_1] = \frac{\text{constant}}{4\pi} \int_{\mathbf{y} \in \Sigma} \frac{\mathbf{n}(\mathbf{y}) \cdot (\mathbf{x} - \mathbf{y})}{|\mathbf{x} - \mathbf{y}|^3} d\Sigma(\mathbf{y}) = \frac{1}{2} v_1. \quad (6)$$

Equation (6) can be interpreted in terms of the solid angle under which Σ can be seen from an arbitrary point located also on Σ . As we will see below, the companion eigenfunction u_1 of \hat{M} is proportional to the equilibrium charge distribution on a conductor of shape determined by Σ . We note that the spectrum of \hat{M} and \hat{M}^\dagger is invariant under the transformation $\mathbf{x} \rightarrow t\mathbf{x}$, $t > 0$ (the scale invariance). In contrast, the spectrum of \hat{S} is proportional to the linear size of Ω . This can be easily checked in the case of a sphere where the eigenvalues of \hat{S} are proportional to the radius of the sphere. Thus, because of \hat{S} , u_i and v_i are not scale invariant. Therefore, the norms of u_i and v_i are proportional to the square-root and to the inverse of the square-root of the linear size of Ω , respectively. The size-dependence of u_i and v_i is also reflected in the bi-orthogonality conditions defined in Ref. [6]. Operators (1)-(3) can be used in the resolution of many physical problems. Dielectric spectra of living cells in microwave and radio-frequency regimes [5, 23] or plasmonic properties of metallic nanoparticles [6, 7, 8, 24, 25] can be treated with the help of \hat{M} and \hat{M}^\dagger whose inversion is carried out via the eigenfunctions u_i and v_i and the corresponding eigenvalues χ_i . However, the above problems do not require normalized eigenfunctions because u_i and v_i come in pairs in the desired solutions [5, 6, 7, 8, 23, 24, 25]. Thus, there is no need for explicit calculation of \hat{S} . Operator \hat{S} is used whenever an explicit expression for the near-field properties like the near-field enhancement produced by localized plasmon resonances are needed [25]. Another example where \hat{S} would be needed is the calculation of capacitance and of equilibrium charge on a metallic object. The Robin problem of finding the equilibrium charge distribution on a conductor of arbitrary shape can be cast into the operator form as [9]

$$\hat{M}[u_R] = \frac{1}{2}u_R(\mathbf{x}), \quad (7)$$

with the constraint $\int_{\mathbf{x} \in \Sigma} u_R(\mathbf{x}) d\Sigma(\mathbf{x}) = 1$. The constraint (normalization condition) can be put in the following form

$$\langle 1 | u_R \rangle = 1, \quad (8)$$

where $1 \in L^2(\Sigma)$ is the constant distribution that has the value 1 on Σ . Equation (7) is found from the jump formula obeyed by the derivative of the single-layer potential across Σ [2] and it has the obvious solution $u_R \propto u_1$. In other words, the solution of Robin problem is proportional to the

eigenfunction of the largest eigenvalue of \hat{M} . The constant value V_R of the electric potential generated by u_R is formally given by

$$\hat{S}[u_R] = V_R 1 \quad (9)$$

and it is called the Robin constant, while its inverse is the capacitance C of the body bounded by Σ [1]. The left-side hand of Eq. (9) needs to be divided by dielectric permittivity ε of the embedding medium if any physical situation is considered. Thus, from (8) and (9), in the general case of an outer medium with dielectric permittivity ε , the capacitance is:

$$C = \frac{1}{V_R} = \frac{\varepsilon}{\langle u_R | \hat{S}[u_R] \rangle}. \quad (10)$$

The quantity $W_{u_R} = \langle u_R | \hat{S}[u_R] \rangle / (2\varepsilon)$ is just the electrostatic energy of the charged metallic body with charge density u_R . The electrostatic energy W_{u_R} of the equilibrium charge density u_R is the energy minimum attained for the set of arbitrary surface charge densities that satisfy the constraint provided by Eq. (8). This is the Thomson theorem [26] and it is used as the definition for the equilibrium charge distribution in abstract mathematical terms [1]. The proof is as follows. For any surface density u one has the expansion $u = \sum_{i=1}^{\infty} a_i u_i$, where a_i are the expansion coefficients of the surface density u . In addition, u obeys $\langle 1 | u \rangle = 1$, which fixes the first expansion coefficient since $\langle 1 | u_i \rangle = 0$ for $i \neq 1$ (the biorthogonality condition). One can prove that the constant a_1 is the proportionality factor between v_1 and the constant distribution 1, i. e., $1 = v_1/a_1$. Thus

$$\begin{aligned} \langle u | \hat{S}[u] \rangle &= \sum_{i,j=1}^{\infty} \langle a_i^* u_i | \hat{S}[a_j u_j] \rangle = \\ &= \sum_{i,j=1}^{\infty} a_i^* a_j \langle u_i | v_j \rangle = \sum_{i,j=1}^{\infty} a_i^* a_j \delta_{ij} = \\ &= \sum_{i=1}^{\infty} |a_i|^2 \geq |a_1|^2 = \langle u_R | \hat{S}[u_R] \rangle. \end{aligned} \quad (11)$$

which demonstrates the Thomson theorem. Moreover, the explicit expression of the equilibrium distribution is

$$u_R = a_1 u_1 \quad (12)$$

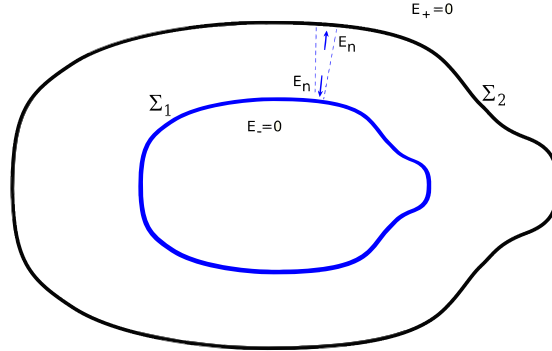


Figure 1: (Color online) Schematic representation of a capacitor with the configurations of fields inside Σ_1 and outside Σ_2 . The dotted lines delimitate a Gaussian surface that is used further in the main text by invoking the Gauss law.

and a_1 is related to the norm of v_1 by

$$\langle v_1 | v_1 \rangle = \|v_1\|^2 = a_1^2 \langle 1 | 1 \rangle = a_1^2 A, \quad (13)$$

where A is the area of Σ . Finally, considering Eqs. (12) and (13) the capacitance expression (10) takes a simple and compact form

$$C = \frac{\varepsilon A}{\|v_1\|^2}. \quad (14)$$

We have pointed out earlier that $\|v_1\|^2$ is proportional to the linear size of Ω , therefore the capacitance itself is also proportional to the linear size of the body. Equation (14) shows explicitly both the geometric dependence of capacitance of an arbitrarily shaped object and the scale invariance of the shape factor $C/\sqrt{4\pi A}$. The shape factor varies slowly with the conductor shape [27] thus, one can say that $\|v_1\|^2$ is a slowly varying function of the conductor shape. In some cases like that of a cube [28] the capacitance is difficult to compute, but as it is suggested by Eq. (14) operator perturbations can be used to estimate the capacitance of any object [29].

3. Capacitors and their capacitance

The capacitance of an arbitrary object is defined and calculated with respect to infinity where the electric potential is supposed to vanish. In

general, a capacitor consists of two separated conducting bodies. We consider a capacitor that is made of two closed and smooth surfaces Σ_1 and Σ_2 in which Σ_2 encloses Σ_1 (Fig. 1). The capacitor capacitance is defined as the total charge that is held on Σ_1 when the electrical potential is 1 on Σ_1 and 0 on Σ_2 . This definition can be cast in a form in which the total charge on Σ_1 is given by the Gauss law or by the total electrostatic energy enclosed within the space between Σ_1 and Σ_2 [26]. The electrostatic problem of a capacitor is to find a function that is 1 on Σ_1 and 0 on Σ_2 and obeys the Laplace equation in the space Ω_{12} between Σ_1 and Σ_2 :

$$\begin{aligned}\Delta u(\mathbf{x}) &= 0; \mathbf{x} \in \Omega_{12} \\ u(\mathbf{x}) &= 1; \mathbf{x} \in \Sigma_1 \\ u(\mathbf{x}) &= 0; \mathbf{x} \in \Sigma_2.\end{aligned}\tag{15}$$

It is easy to see that, with the boundary condition taken from (15), the solution of the Laplace equation inside of Σ_1 and outside of Σ_2 is the constant 1 and the constant 0, respectively. Inside Ω_{12} we seek a solution for (15) in the form of two single-layer potentials

$$u(x) = \frac{1}{4\pi} \int_{\mathbf{y} \in \Sigma_1} \frac{\mu_1(\mathbf{y})}{|\mathbf{x} - \mathbf{y}|} d\Sigma(\mathbf{y}) + \frac{1}{4\pi} \int_{\mathbf{y} \in \Sigma_2} \frac{\mu_2(\mathbf{y})}{|\mathbf{x} - \mathbf{y}|} d\Sigma(\mathbf{y}),\tag{16}$$

where μ_1 and μ_2 are the induced charge densities on Σ_1 and Σ_2 . Similar to (1) we define on Σ_1 and Σ_2 four operators \hat{M}_{11} , \hat{M}_{12} , \hat{M}_{21} , and \hat{M}_{22} as

$$\hat{M}_{ij}[\mu_j] = \frac{1}{4\pi} \int_{\mathbf{x} \in \Sigma_i, \mathbf{y} \in \Sigma_j} \frac{\mu_j(\mathbf{y}) \mathbf{n}(\mathbf{x}) \cdot (\mathbf{x} - \mathbf{y})}{|\mathbf{x} - \mathbf{y}|^3} d\Sigma(\mathbf{y}),\tag{17}$$

with $i, j = \overline{1, 2}$. The equations obeyed by μ_1 and μ_2 are

$$\begin{aligned}\hat{M}_{11}[\mu_1] + \hat{M}_{12}[\mu_2] &= \frac{1}{2}\mu_1 \\ \hat{M}_{21}[\mu_1] + \hat{M}_{22}[\mu_2] &= -\frac{1}{2}\mu_2,\end{aligned}\tag{18}$$

which say that the normal fields on Σ_1 from inside and on Σ_2 from outside are zero. The solution of (18) is the solution of (15) up to a multiplicative constant. The multiplicative constant is fixed by the equations that set the boundary conditions of (15):

$$\begin{aligned}\hat{S}_{11}[\mu_1] + \hat{S}_{12}[\mu_2] &= 1 \\ \hat{S}_{21}[\mu_1] + \hat{S}_{22}[\mu_2] &= 0,\end{aligned}\tag{19}$$

with \hat{S}_{ij} being similar to (3)

$$\hat{S}_{ij}[u] = \frac{1}{4\pi} \int_{\mathbf{x} \in \Sigma_i, \mathbf{y} \in \Sigma_j} \frac{u(\mathbf{y})}{|\mathbf{x} - \mathbf{y}|} d\Sigma(\mathbf{y}). \quad (20)$$

The capacitance of the capacitor is the total charge represented by charge density μ_1 and depends not only on operators like (1) and (2) but also on inter-surface operators (17). In the special case when Σ_2 is an equipotential surface determined by the equilibrium charge distributed on Σ_1 a compact formula based on operators (1)-(2) can be deduced for capacitance. It is not hard to see that Eqs. (18) have as solutions the charge densities μ_1 and μ_2 , which are proportional to the equilibrium charge densities induced on Σ_1 and Σ_2 , respectively. In addition, μ_1 and μ_2 must have opposite signs. To determine μ_1 and μ_2 , and the capacitor capacitance one needs also Eqs. (19). Thus, by integrating the first equation of (19) on Σ_1 and the second equation on Σ_2 one obtains the following relations

$$\begin{aligned} V_1 + V_2 &= 1 \\ V_{12} + V_2 &= 0 \end{aligned} \quad (21)$$

where V_1 is the electric potential induced by μ_1 on Σ_1 , V_2 is the electric potential induced by μ_2 inside Σ_2 as well as on Σ_1 , and V_{12} is the electric potential induced on Σ_2 by μ_1 . On the other hand, the total charge is

$$Q_1 = \int_{\mathbf{x} \in \Sigma_1} \mu_1(\mathbf{x}) d\Sigma_1(\mathbf{x}) = C_1 V_1 \quad (22)$$

on Σ_1 and

$$Q_2 = \int_{\mathbf{x} \in \Sigma_2} \mu_2(\mathbf{x}) d\Sigma_2(\mathbf{x}) = C_2 V_2 \quad (23)$$

on Σ_2 . We mention that Eqs. (22) and (23) are valid only whenever Σ_2 is one of the equipotential surfaces determined by an equilibrium charge distributed on Σ_1 . Equation (14) provides the expressions of C_1 and C_2 that are the capacitances of Σ_1 and Σ_2 , respectively. Moreover

$$Q_1 + Q_2 = 0 \quad (24)$$

which is the Gauss law that is obtained from the second equation of (18). Combining Eqs. (21), (22), (23), and (24) we obtain the capacitor capacity

$$C_{cond} = \left(\frac{1}{C_1} - \frac{1}{C_2} \right)^{-1}. \quad (25)$$

Particular examples in which Eq. (25) is directly applicable is the capacitance of concentric spheres and of a coaxial cable. For a capacitor made of two concentric spheres the capacitance is $C_{sph_cond} = \frac{4\pi\epsilon R_1 R_2}{R_2 - R_1}$, where R_1 and R_2 are the radii of the two spheres with $R_2 > R_1$. Having in mind the capacitance of a sphere as $C_{sph} = 4\pi\epsilon R$, it is easy to check that C_{sph_cond} has the form given by Eq. (25). Moreover, the capacitance of a capacitor made of two confocal spheroids obeys also (25), with C_1 and C_2 as having analytic expressions that are given in the standard textbooks of classical electrodynamics [26].

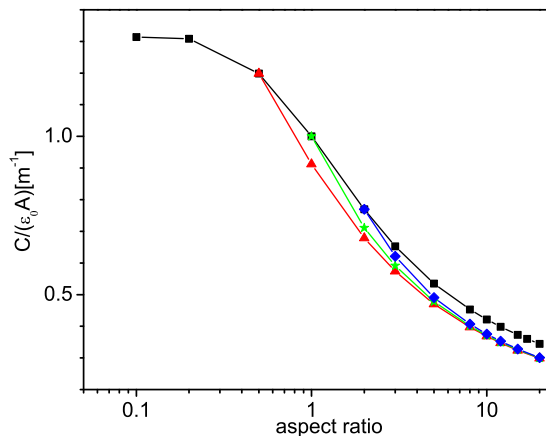


Figure 2: (Color online) Calculated capacitance per unit area versus aspect ratio for spheroids (black squares) and for cylindrical rods with different end-cap geometries: oblate spheroid (red triangles), sphere (green stars), and prolate spheroid (blue diamonds). It is assumed that the largest cross-sectional radius is 1 m.

4. A Numerical method. Discussion

As we have previously discussed, capacitance can be determined in numerical simulators used to calculate other physical properties like the localized

plasmon resonances in metallic nanoparticles [6, 7, 8]. The method is an operator based BIE method that calculates numerically the eigenvalues χ_k and the eigenvectors u_k and v_k of \hat{M} and \hat{M}^\dagger , respectively. In order to have normed u_k and v_k one needs also to calculate the matrix elements of \hat{S} [25]. The method belongs to the class of the spectral methods, where the functions of the basis set are defined globally rather than locally like in the FEM [30]. Details of the method for axisymmetric objects are given in Refs. [23, 24]. We have performed calculations for oblate and prolate spheroids as well as for cylindrical rods with different end-cap geometries: half of an oblate spheroid with 1/2 aspect ratio, half of a sphere, and half of a prolate spheroid with an aspect ratio of 2. To set the input data we have considered that the largest cross-sectional radius is 1 m for all the above geometries. The aspect ratio of any considered object is the ratio between the largest axial length and the largest cross-sectional diameter. The results are given in Fig. 2, where the capacitance per unit area is plotted. For the same aspect ratio the rods have larger capacitances than the spheroids. Moreover, for aspect ratios greater than 5 the capacitance of the rods do not depend any longer on the end-cap geometry.

Our numerical calculations show a very good agreement with the analytical results for spheroidal shapes which can be found in Refs. [26]. The relative error is at least 5×10^{-5} with a relative small overhead of 25 functions in the basis and 96 quadrature points. We have also checked these results against the more sophisticated Trefftz based FEM calculations provided by the multi-physics program ANSYS [31]. The relative error in this case is around 10^{-2} (about 1% and two order of magnitude greater than the BIE results). In ANSYS the capacitance results obtained with the Trefftz method are much better than the results obtained by using infinite elements. On the other hand, we compared the BIE calculations with ANSYS Trefftz calculations for the rods and the two calculations are apart by less than 1%. An example of rods with finite length is that of capped carbon nanotubes which are used as electrochemical double-layer capacitors (supercapacitors) for energy storage [32]. The implementation of BIE for axisymmetric shapes has also shown to provide very accurate results of the depolarization factors which are related to the other eigenvalues of \hat{M} and \hat{M}^\dagger [33].

A direct application of these calculations is the estimation of membrane capacitance in living cells. The shelled ellipsoidal model is one of the most common models of living cells in modeling dielectric spectroscopy experiments [34]. In the ellipsoidal shelled model the shell designates the cell

membrane that is bounded by two confocal ellipsoids and it is practically non-conductive in radiofrequency. Living cells accumulates positive/negative charge on the outer/inner surface of the membrane, giving rise to a resting potential across the membrane. In dielectric spectra the charge on the membrane is responsible for the α -relaxation (usually below the frequency of 10 KHz), whilst the dielectric mismatch between the cell and the surrounding medium gives rise to β -relaxation in the MHz range of the radiofrequency spectrum [35]. The cell resting potential may be an input parameter in theoretical analysis of both α - and β -relaxations, thus the membrane capacitance needs to be estimated [36, 37]. In the spherical model of living cells Prodan et al. [37] used the expression of a parallel-plane capacitor for the normalized capacitance (capacitance divided by area). It turns out that the formula of a parallel-plane capacitor is very close to that of a spherical living cell. The cell membrane is very thin with respect to the overall size of the cell, hence, for a spherical model of living cells, the membrane capacitance is approximated by

$$C_{sph_membr} \approx \varepsilon A_2/d = C_2/(\delta - 1), \quad (26)$$

where $d = R_2 - R_1$, with R_1 and R_2 as the inner and outer membrane radius of areas A_1 and A_2 , respectively. C_2 is capacitance of the outer sphere and $\delta = R_2/R_1 > 1$ obeys the condition $(\delta - 1) \ll 1$. In the general case of arbitrarily shaped cells the parallel-plane capacitor formula cannot be used anymore although intuition may suggest otherwise. An analytical formula for the membrane capacitance of spheroidal living cells is provided by the combination of capacitance formula for spheroids [26] and Eq. 25.

In Fig. 3 there are presented two shape factors that are related to capacitance and are scale-invariant. These shape factors can be straightforwardly utilized in approximate capacitance calculations for metallic object of various shapes. The first scale-invariant shape factor ($= A^{1/2}/(2\pi^{1/2}||v_1||^2)$) is related to the area of the object (Fig. 3a) and it shows a relative shape insensitivity for aspect ratios less than 5. This shape factor has been used in isoperimetric inequalities to estimates the capacitance of objects with shapes close to the spherical shape [27]. In fact, Chow and Yovanovich noticed that this shape factor varies little over a wide range of shapes.

The second scale-invariant shape factor related to capacitance is $V^{1/3}/||v_1||^2$. It is defined by using the volume of the object and shows shape insensitivity for long structures (Fig. 3b). Thus for an aspect ratio greater than 5 the

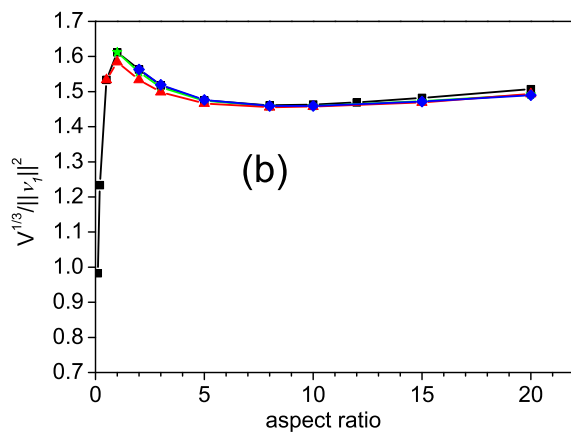
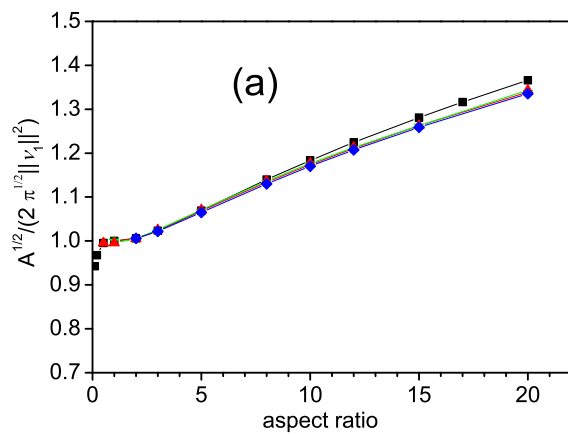


Figure 3: (Color on-line) Scale-invariant shape factors versus aspect ratio. The shape factors are defined (a) by the area of the object and (b) by its volume. The spheroids are denoted by black squares and the cylindrical rods with different end-cap geometries are depicted by red triangles (oblate spheroid end-cap), by green stars (spherical end-cap), and by blue diamonds (prolate spheroid end-cap).

rods and the spheroids have almost the same volume related shape factors, which also vary little not only with the shape but also with respect to the aspect ratio. We note here that quantum capacitance of molecular nanowires is scaling with $V^{1/3}$ rather than with the length of the nanowire [38], thus for long structures the volume rather than the area of the object plays a greater role in determining the capacitance of an object.

5. Summary and Conclusions

We have presented a very compact formula of the capacitance for an arbitrarily shaped metallic object. Capacitance can be calculated with the help of the Neumann-Poincaré operator, which together with its adjoint plays a central role in the resolution of elliptic partial differential equations like the Laplace equation. The formula of capacitance is stated simply as follows. The capacitance is direct proportional to the dielectric permittivity of the embedding medium and to the area of the object, and inverse proportional to the squared norm of the eigenfunction of the Neumann-Poincaré operator with the largest eigenvalue. The operator approach on capacitance permits an elegant proof of the Thomson theorem which says that the electrostatic energy accumulated on a metallic body reaches its minimum when the charge distribution on the body is in equilibrium. In addition, the capacitance and the charge distribution on a metallic object is a byproduct obtained in BIE numerical simulators of localized plasmon resonances.

We have shown also how the capacitance of a capacitor can be related to the individual capacitance of each surface of the capacitor. Thus, when the outer surface of the capacitor is an equipotential surface generated by the charging of the inner surface then the capacitor behaves like a series capacitor with the total capacitance as being the capacitance of the inner surface in series with the opposite (negative) capacitance of the outer surface of the capacitor. These results have been used in the analysis of membrane capacitance in living cells, where the parallel-plane capacitor model works for spherical cells but is not appropriate for membrane capacitance of arbitrarily shaped living cells.

The capacitance formula allows us to define scale-invariant shape factors that can be used in the approximate calculation of capacitance. We have analyzed two scale-invariant shape factors. One of the shape factors employs the volume of the object and is more suitable for long shapes like rods or

wires. Alternatively, the other shape factor, which is defined in terms of the object area, is appropriate for objects with shapes close to a sphere.

6. Acknowledgments

This work was supported by a grant of the Romanian National Authority for Scientific Research, CNCS – UEFISCDI, project number PNII-ID-PCCE-2011 -2-0069.

References

- [1] O. D. Kellog, Foundations of Potential Theory, Springer-Verlag, Berlin-Heidelberg-New York, 1967.
- [2] D. Khavinson, M. Putinar, H. S. Shapiro, Arch. Ration. Mech. Anal. 185 (2007) 143.
- [3] N. Günter, La theorie du potentiel et ses applications aux problemes fondamentaux de la physique mathematique, Gauthier-Villars, Paris, 1934.
- [4] D. J. Bergman, Phys Rep. 43 (1978) 377.
- [5] D. Vrinceanu, E. Gheorghiu, Bioelectrochem. Bioenerg. 40 (1996) 167.
- [6] F. Ouyang, M. Isaacson, Philos. Mag. B 60 (1989) 481.
- [7] I. D. Mayergoyz, D. R. Fredkin, Z. Zhang, Phys. Rev. B 72 (2005) 155412.
- [8] T. J. Davis, K. C. Vernon, D. E. Gomez, Phys. Rev. B 79 (2009) 155423.
- [9] J. G. Van Bladel, Electromagnetic Fields, Wiley-Interscience, Hoboken, New Jersey, 2007.
- [10] T. Simonson, Rep. Prog. Phys. 66 (2003) 737.
- [11] W. A. Hofer, A. S. Foster, A. L. Shluger, Rev. Mod. Phys. 75 (2003) 1287.
- [12] S. Hudlet, M. S. Jean, C. Guthmann, J. Berger, Eur. Phys. J. B 2 (1998) 5.

- [13] P. Simon, Y. Gogotsi, *Nature Mat.* 7 (2008) 845.
- [14] J. B. Hubbard, J. F. Douglas, *Phys. Rev. E* 47 (1993) R2983.
- [15] J. F. Douglas, H. X. Zhou, J. B. Hubbard, *Phys. Rev. E* 49 (1994) 5319.
- [16] M. Mascagnia, N. A. Simonov, *J. Comput. Phys.* 195 (2004) 465.
- [17] C. Johnson, *Numerical Solutions of Partial Differential Equations by Finite Element Method*, Cambridge Univ. Press, Cambridge, 1987.
- [18] D. Poljak, C. A. Brebbia, *Boundary Element Methods for Electrical Engineers*, WIT, Boston, 2005.
- [19] P. Bettess, *Int. J. Numer. Methods Eng.* 11 (1977) 53.
- [20] D. A. Lowther, E. M. Freeman, B. Forghani, *IEEE Trans. Magn.* 25 (1989) 2810.
- [21] S. J. Salon, J. D'Angelo, *IEEE Trans. Magn.* 24 (1988) 80.
- [22] Q. H. Qin, *Appl. Mech. Reviews* 58 (2005) 316.
- [23] T. Sandu, D. Vrinceanu, E. Gheorghiu, *Phys. Rev. E* 81 (2010) 021913.
- [24] T. Sandu, D. Vrinceanu, E. Gheorghiu, *Plasmonics* 6 (2011) 407.
- [25] T. Sandu, *Plasmonics* xx (2013) xxx, doi:10.1007/s11468-012-9403-z.
- [26] L. D. Landau, E. M. Lifshitz, *Electrodynamics of Continuous Media*, Pergamon, Oxford-New York, 1984.
- [27] Y. L. Chow, M. M. Yovanovich, *J. Appl. Phys.* 53 (1982) 8470.
- [28] C. O. Hwang, M. Mascagni, *J. Appl. Phys.* 95 (2004) 3798.
- [29] D. Grieser, H. Uecker, S. A. Biehs, O. Huth, F. Rütting, M. Holthaus, *Phys. Rev. B* 80 (2009) 245405.
- [30] J. P. Boyd, *Chebyshev and Fourier Spectral Methods*, Dover, New York, 2001.
- [31] www.ansys.com

- [32] J. Huang, B. G. Sumpter, V. Meunier, G. Yushin, C. Portet, Y. Gogotsi, *J. Mater. Res.* 25 (2010) 1525.
- [33] T. Sandu, *J. Nanopart. Res.* 14 (2012) 905.
- [34] K. Asami, T. Hanai, N. Koizumi, *Jpn. J. Appl. Phys.* 19 (1980) 359.
- [35] R. Stoy, K. Foster, H. Schwan, *Phys. Med. Biol.* 27 (1982) 501.
- [36] C. Prodan, E. Prodan, *J. Phys. D: Appl. Phys.* 32 (1999) 335.
- [37] E. Prodan, C. Prodan, , J. H. Miller, *Biophys. J.* 95 (2008) 4174.
- [38] J. C. Ellenbogen, C. A. Picconatto, J. S. Burnim, *Phys. Rev. A* 75 (2007) 042102.